Mol Genet Genomics (2009) 282:257–271
DOI 10.1007/s00438-009-0463-5

ORIGINAL PAPER

Functional analysis and subcellular localization of two geranylgeranyl diphosphate synthases from *Penicillium paxilli*

Sanjay Saikia · Barry Scott

Received: 12 January 2009 / Accepted: 28 May 2009 / Published online: 16 June 2009

Abstract The filamentous fungus *Penicillium paxilli* contains two distinct geranylgeranyl diphosphate (GGPP) synthases, GgsA and GgsB (PaxG). PaxG and its homologues in *Neotyphodium lolii* and *Fusarium fujikuroi* are associated with diterpene secondary metabolite gene clusters. The genomes of other filamentous fungi including *Aspergillus fumigatus*, *Aspergillus nidulans*, *Aspergillus niger*, *Aspergillus oryzae* and *Fusarium graminearum* also contain two or more copies of GGPP synthase genes, although the diterpene metabolite capability of these fungi is not known. The objective of this study was to understand the biological significance of the presence of two copies of GGPP synthases in *P. paxilli* by investigating their subcellular localization. Using a carotenoid complementation assay and gene deletion analysis, we show that *P. paxilli* GgsA and PaxG have GGPP synthase activities and that *paxG* is required for paxilline biosynthesis, respectively. In the Δ*paxG* mutant background *ggsA* was unable to complement paxilline biosynthesis. A GgsA-EGFP fusion protein was localized to punctuate organelles and the EGFP-GRV fusion protein, containing the C-terminus tripeptide GRV of PaxG, was localized to peroxisomes. A truncated PaxG mutant lacking the C-terminus tripeptide GRV was unable to complement a Δ*paxG* mutant demonstrating that the tripeptide is functionally important for paxilline biosynthesis.

Keywords Geranylgeranyl diphosphate synthase · Subcellular localization · Peroxisome · Indole-diterpene · Secondary metabolism · *Penicillium paxilli*

Communicated by R. Fischer.

Electronic supplementary material The online version of this article (doi:10.1007/s00438-009-0463-5) contains supplementary material, which is available to authorized users.

S. Saikia · B. Scott (✉)
Institute of Molecular Biosciences, Massey University,
Private Bag 11 222, Palmerston North, New Zealand
e-mail: d.b.scott@massey.ac.nz

Present Address:
S. Saikia
Michael Smith Laboratories,
The University of British Columbia,
Vancouver, BC V6T 1Z4, Canada
e-mail: ssaikia@msl.ubc.ca

Introduction

Geranylgeranyl diphosphate (GGPP) synthases belong to the prenyltransferase family that catalyze the sequential addition of isopentenyl diphosphate (IPP) to allylic prenyl diphosphates, forming products of varying chain-lengths and double-bond stereochemistry that are specific to each enzyme. In eukaryotes, GGPP synthases catalyze the synthesis of GGPP predominantly in a single step reaction from farnesyl diphosphate (FPP) and IPP, or alternatively, in a series of reactions involving the addition of IPP to dimethylallyl diphosphate, geranyl diphosphate, and FPP. Genes encoding GGPP synthases have been isolated from various organisms. These GGPP synthases contain five conserved regions including the two aspartate-rich DDXX(XX)D and DDXXD motifs that are implicated in binding of the diphosphate moiety of the allylic substrates through Mg^{2+} ions (Chen et al. 1994).

GGPP synthase is a key branch-point enzyme that produces the precursor GGPP for various isoprenoids including

carotenoids, chlorophylls and diterpenes, and also for protein prenylation mediated by geranylgeranyl transferase. In most eukaryotes, the GGPP precursors are derived from the mevalonate pathway using acetyl-CoA as the primary substrate. These precursors are found in different subcellular compartments including mitochondria, peroxisomes, endoplasmic reticulum and cytosol (Daum et al. 1998; Kovacs et al. 2007), implying compartmentalization of the corresponding enzymes. The sorting of enzymes to different organelles depends on the presence of targeting and sorting signals within their amino acid sequences (Verner and Schatz 1988).

Although compartmentalization of primary metabolic pathways is well recognized in fungal cell, very few studies have been carried out that demonstrate the contribution of compartmentalization to secondary metabolism. Among these is the well-studied pathway of penicillin biosynthesis by the filamentous fungus *Penicillium chrysogenum* wherein parts of the pathway have been shown to be carried out in vacuoles and peroxisomes (Lendenfeld et al. 1993; Muller et al. 1991, 1992). These studies highlighted the importance of targeting signals in correct localization of proteins for penicillin biosynthesis. When the C-terminal peroxisomal targeting signal type 1 (PTS1)-like tripeptide ARL of the acyltransferase enzyme, involved in penicillin biosynthesis, was truncated, it was not targeted to peroxisomes, and transformants expressing the truncated protein did not produce penicillin (Muller et al. 1992). In addition, an aryl-capping enzyme that supplies an activated substrate to the acyltransferase also contains a PTS1 motif, indicating the presence of a functional complex for penicillin biosynthesis in peroxisomes (Lamas-Maceiras et al. 2006). The involvement of peroxisomes in secondary metabolite biosynthesis has also been suggested for proteins involved in AK-toxin biosynthesis in *Alternaria alternata* (Tanaka et al. 1999; Tanaka and Tsuge 2000). In *Aspergillus* species, localization studies have shown compartmentalization of the aflatoxin biosynthesis pathway in the cytoplasm, vacuoles, endoplasmic reticulum-like structures and peroxisomes (Chiou et al. 2004; Lee et al. 2004; Maggio-Hall et al. 2005). However, such studies have not been undertaken on diterpene secondary metabolic pathways.

The diterpene producing filamentous fungi viz., *Penicillium paxilli*, *Neotyphodium lolii* and *Fusarium fujikuroi*, contain two copies of genes that encode GGPP synthases, one of which is associated with secondary metabolite gene clusters for paxilline, lolitrem and gibberellin biosynthesis, respectively, (Tudzynski and Holter 1998; Young et al. 2001, 2005). This led us to hypothesize that the biosynthetic pathways utilizing these enzymes might be compartmentalized. In this study, we tested our hypothesis by investigating the subcellular localization of the two *P. paxilli* GGPP synthases, GgsA and PaxG.

Materials and methods

Strains, media and plasmids

P. paxilli and bacterial strains used in this study are listed in Table 1. *Escherichia coli* strain DH5α (Invitrogen) served as the host for routine cloning. The transformants of this host were grown on LB agar plates supplemented with ampicillin (100 μg/ml) for selection. Cultures of wild-type *P. paxilli* Bainier (PN2013 = ATCC26601) (Itoh et al. 1994) and its derivatives were routinely grown in *Aspergillus* complete medium at 22°C for 4–6 days as described previously (Saikia et al. 2007). Fungal cultures used for the isolation of genomic DNA, RNA, preparation of protoplasts and indole-diterpene analysis were also grown as described previously (Saikia et al. 2007). Fungal cultures used for microscopy were grown on 2.4% PD (potato dextrose) agar or PD agar supplemented with oleic acid (5 mM) at 22°C for approximately 2 days.

Preparation of DNA, hybridizations and PCR

Fungal genomic DNA was isolated from freeze-dried mycelium using a modification of the method of Yoder (Yoder 1988) as described previously (Young et al. 1998). Plasmid DNA was isolated and purified by alkaline lysis using a High Pure Plasmid Isolation Kit (Roche Applied Science). DNA fragments and PCR products were purified using Wizard® SV Gel and PCR Clean-Up System (Promega). Genomic digests were transferred to positively charged nylon membranes (Roche Applied Science) by capillary transfer (Southern 1975) and DNA fixed by UV light cross-linking in a Cex-800 Ultra-Lum Electronic UV Crosslinker (Ultra-Lum Inc, Paramount, CA, USA) at 254 nm for 2 min. Filters were probed with [α-^{32}P]-dCTP (3,000 Ci/mmol, Amersham Biosciences) labeled probes. DNA was labeled by primed synthesis with Klenow polymerase using a High Prime kit (Roche Applied Science). Hybridizations were carried out at 65°C overnight in a hybridization solution (3× SSC) and membranes were washed and hybridization signals detected by autoradiography as described previously (Young et al. 1998).

PCR of genomic DNA for cloning was carried out in a 25 μl reaction volume containing 1× reaction buffer (Roche Applied Science), a 200 μM concentration of each dNTP, a 300 nM concentration of each primer and 2.6 U of Expand High Fidelity Enzyme Mix (Roche Applied Science). Standard PCR of plasmid DNA and PCR screening for cloned genes was carried out in a 50 μl reaction volume containing 1× reaction buffer (Roche Applied Science), a 100 μM concentration of each dNTP, a 200 nM concentration of each primer and 2 U of Taq DNA polymerase (Roche Applied Science).

Table 1 Strains and plasmids

Strains and plasmids	Plasmid/identifier	Relevant characteristics[a]	Source/References
Plasmids			
pGEM®-T Easy		Amp^R	Promega
pGEX-6P-3		Amp^R	Amersham Biosciences
pSP72		Amp^R	Promega
	pACCAR25ΔcrtE	Chl^R(*crtZ-crtB-crtI-crtY-crtX* of *Erwinia uredovora*)	Sandmann et al. 1993
	pCB1004	Hyg^R/Chl^R	Carroll et al. 1994
	pPgpd-DsRed	Amp^R	Mikkelsen et al. 2003
	pII99	Amp^R/Gen^R	Namiki et al. 2001
pPN1851		Amp^R	Young et al. 2006
pPN94		Amp^R/Hyg^R	Takemoto et al. 2006
pPN97		pPN94 containing *EGFP*-cDNA on a 0.72-kb *X*bal/*Not*l fragment; Amp^R/Hyg^R	Aiko Tanaka
	pSF 15.15	Amp^R/Hyg^R (P*trpC-hph*-T*trpC*)	Simon Foster
	pSF 16.17	Amp^R/Gen^R (P*trpC-nptII*-T*trpC*)	Simon Foster
	pSS8	Amp^R/Gen^R	Saikia et al. 2006
	pSS16	Amp^R/Gen^R	Saikia et al. 2006
	pSS27	pPN94 containing *paxG-EGFP* cDNA; Amp^R/Hyg^R	This study
	pSS28	pPN94 containing *EGFP-paxG* cDNA; Amp^R/Hyg^R	This study
	pSS29	pPN94 containing *ggsA-EGFP* cDNA; Amp^R/Hyg^R	This study
	pSS30	pPN94 containing *EGFP-ggsA* cDNA; Amp^R/Hyg^R	This study
	pSS37	pSF 16.17 containing P*TEF*-T*trpC* on a 1.4-kb *Sa*/l/*Bg*/ll fragment; Amp^R/Gen^R	This study
	pSS41	pSS37 containing *DsRed*-SKL cDNA; Amp^R/Gen^R	This study
	pSS46	pPN94 containing *EGFP*-GRV cDNA; Amp^R/Hyg^R	This study
	pSS52	pSF 15.15 containing 1.04-kb *Sa*/l/*Hin*dlll and 1.0-kb *Eco*RV/*Sac*I fragments 5′ and 3′ of *paxG*; Amp^R/Hyg^R	This study
	pSS54	pPN94 containing *EGFP-N*368*paxG* cDNA; Amp^R/Hyg^R	This study
	pSS64	pGEX-6P-3 containing *paxG* cDNA on a 1.13-kb *Bam*Hl/*Xho*l fragment; Amp^R	This study
	pSS65	pGEX-6P-3 containing *ggsA* cDNA on a 1.14-kb *Bam*Hl/*Xho*l fragment; Amp^R	This study
	pSS66	pGEX-6P-3 containing truncated *ggs*A cDNA on a 1.04-kb *Bam*Hl/*Xho*l fragment; Amp^R	This study
	pSS68	pGEX-6P-3 containing truncated *ggsA* cDNA on a 0.93-kb *Bam*Hl/*Xho*l fragment; Amp^R	This study
	pSS75	pII99 containing full-length *paxG* on a 1.93-kb *Hin*dlll/*Xho*l fragment; Amp^R/Gen^R	This study
	pSS89	pGEX-6P-3 containing truncated *ggsA* cDNA on a 0.91-kb *Bam*Hl/*Xho*l fragment; Amp^R	This study
	pSS110	pPN1851 containing full-length *paxG* on a 1.30-kb *Nco*l/*Kpn*l fragment; Amp^R/Hyg^R	This study
	pSS111	pPN1851 containing truncated paxG on a 1.29-kb *Nco*l/*Kpn*l fragment; Amp^R/Hyg^R	This study
	pSS112	pPN1851 containing full-length *ggsA* with added SKL at C-terminus on a 1.23-kb *Nco*l/*Kpn*l fragment; Amp^R/Hyg^R	This study
	pSS113	pPN1851 containing truncated *ggsA* with added SKL at C-terminus on a 1.01-kb *Nco*l/*Kpn*l fragment; Amp^R/Hyg^R	This study

Table 1 continued

Strains and plasmids	Plasmid/identifier	Relevant characteristics[a]	Source/References
Fungal strains (P. *paxilli*)			
PN2013		Wild type; paxilline positive	Itoh et al. 1994
PN2549	WT/pSS30-T5	PN2013/pSS30; P*TEF-EGFP-ggsA*-T*trpC*; Hyg^R; paxilline positive	This study
PN2555	WT/pSS29-T12	PN2013/pSS29; P*TEF-ggsA-EGFP*-T*trpC*; Hyg^R; paxilline positive	This study
PN2559	WT/pSS27-T13	PN2013/pSS27; P*TEF-paxG-EGFP*-T*trpC*; Hyg^R; paxilline positive	This study
PN2564	WT/pSS46-T10	PN2013/pSS46; P*TEF-EGFP*-GRV-T*trpC*; Hyg^R; paxilline positive	This study
PN2566	WT/pSS41-T1	PN2013/pSS41; P*TEF-DSRed-SKL*-T*trpC*; Gen^R; paxilline positive	This study
PN2570	WT/pSS41-T1/ pSS46-T4	PN2566/pSS46; P*TEF-DsRed*-SKL-T*trpC/PTEF-EGFP*-GRV-T*trpC*; Gen^R/Hyg^R; paxilline positive	This study
PN2575	WT/pSS29-T12/ pSS41-T1	PN2555/pSS41; P*TEF-ggsA-EGFP*-T*trpC/PTEF-DsRed*-SKL-T*trpC*; Hyg^R/Gen^R; paxilline positive	This study
PN2662	SSG2	PN2013/pSS52; Δ*paxG*, Hyg^R; paxilline negative	This study
PN2663	SSG2/pSS75-T3	PN2662/pSS75; Hyg^R/Gen^R; paxilline positive	This study
PN2664	SSG2/pSS110-T3	PN2662/pSS110; P*pax*M-*pax*G; Hyg^R; paxilline positive	This study
PN2665	SSG2/pSS111-T6	PN2662/pSS111; P*pax*M-N368*pax*G; Hyg^R; paxilline negative	This study
PN2666	SSG2/pSS112-T5	PN2662/pSS112; P*pax*M-*ggsA*-SKL; Hyg^R; paxilline negative	This study
PN2667	SSG2/pSS113-T2	PN2662/pSS113; P*pax*M-C304*ggSA*-SKL; Hyg^R; paxilline negative	This study
PN2731	WT/pSS54-T2	PN2013/pSS54; P*TEF-EGFP*-N368*pax*G-T*trp*C; Hyg^R; paxilline positive	This study
Bacterial strains (*E. coli*)			
BL21 (DE3)		*hsdS gal* (λcl*ts*857 *ind*1 Sam7 *nin*5 *lac*UV5-T7 gene *1*)	Studier and Moffatt 1986
DH5α		*supE*44 Δ*lac*U169 (ϕ80 *lacZ* ΔM15) *hsd*R17 *recA*1 *endA*1 *gyrA*96 *thi*-1 *relA*1	Invitrogen
PN1775		BL21 (DE3)/pACCAR25ΔcrtE	Rohan Lowe
PN4003		DH5α/pSS27	This study
PN4004		DH5α/pSS28	This study
PN4005		DH5α/pSS29	This study
PN4006		DH5α/pSS30	This study
PN4007		DH5α/pSS37	This study
PN4008		DH5α/pSS41	This study
PN4010		DH5α/pSS46	This study
PN4072		DH5α/pSS52	This study
PN4073		DH5α/pSS75	This study
PN4074		DH5α/pSS110	This study
PN4075		DH5α/pSS111	This study
PN4076		DH5α/pSS112	This study
PN4077		DH5α/pSS113	This study
PN4067		PN1775/pSS64	This study
PN4068		PN1775/pSS65	This study
PN4069		PN1775/pSS66	This study
PN4070		PN1775/pSS68	This study
PN4071		PN1775/pSS89	This study
PN4085		DH5α/pSS54	This study

Amp^R ampicillin-resistant, Chl^R chloramphenicol-resistant, Gen^R geneticin-resistant, Hyg^R hygromycin-resistant

The thermocycle conditions routinely used with Expand High Fidelity Enzyme Mix and Taq DNA polymerase were one cycle at 94°C for 2 min, 30 cycles at 94°C for 30 s, 55°C for 30 s, and 72°C for 1 min (per kb) and one cycle at 72°C for 5 min. Reactions were carried out in a Mastercycler® gradient (Eppendorf, Hamburg, Germany) thermocycler.

Preparation of RNA and RT-PCR

Total RNA was isolated from frozen mycelium using TRIzol® reagent (Invitrogen). cDNA was synthesized from total RNA using SuperScript™ First-Strand Synthesis System for RT-PCR (Invitrogen). RT-PCR for expression analysis was performed with 1 µl of cDNA using reactions and thermocycle conditions as described for PCR of genomic DNA for cloning (see above).

Preparation of reporter fusion, deletion and complementation constructs

Plasmids pSS27 (*PaxG-EGFP*) and pSS28 (*EGFP-PaxG*) were prepared to study the subcellular localization of PaxG in the fungal cell. Plasmid pSS27 was prepared by cloning a 1.11-kb *Spe*I/*Xho*I fragment and a 0.72-kb *Xho*I/*Not*I fragment containing the coding regions of *paxG* and *EGFP*, respectively, into pPN94 that contains *TEF* promoter and *trpC* terminator (Takemoto et al. 2006). The *Spe*I/*Xho*I and *Xho*I/*Not*I fragments were prepared by digesting PCR products amplified with primer sets paxG-Sp-F/paxG-Xh-R (Table 2; lists sequences of all primers cited in this study) and EGFP-Xh-F/EGFP-No-R using wild-type cDNA and pPN97 as templates, respectively. Plasmid pPN97 was prepared by cloning a 0.72-kb *Xba*I/*Not*I fragment containing the coding region of *EGFP* into pPN94. Plasmid pSS28 was prepared by cloning a 0.72-kb *Xba*I/*Xho*I fragment and a 1.11-kb *Xho*I/*Not*I fragment containing the coding regions of *EGFP* and *paxG*, respectively, into pPN94. The *Xba*I/*Xho*I and *Xho*I/*Not*I fragments were prepared by digesting PCR products amplified with the primer sets EGFP-Xb-F/EGFP-Xh-R and paxG-Xh-F2/paxG-No-R2 using pPN97 and wild-type cDNA as templates, respectively. Plasmids pSS29 (*GgsA-EGFP*) and pSS30 (*EGFP-GgsA*) were prepared to study the subcellular localization of GgsA in the fungal cell. Plasmid pSS29 was prepared by cloning a 1.12-kb *Xba*I/*Xho*I fragment and a 0.72-kb *Xho*I/*Not*I fragment containing the coding regions of *ggsA* and *EGFP*, respectively, into pPN94. The *Xba*I/*Xho*I and *Xho*I/*Not*I fragments were prepared by digesting PCR products amplified with primer sets ggs1-Xb-F/ggs1-Xh-R and EGFP-Xh-F/EGFP-No-R using wild-type cDNA and pPN97 as templates, respectively. Plasmid pSS30 was prepared by cloning a 0.72-kb *Xba*I/*Xho*I fragment and a 1.12-kb *Xho*I/*Not*I fragment containing the coding regions of *EGFP* and *ggsA*, respectively, into pPN94. The *Xba*I/*Xho*I and *Xho*I/*Not*I fragments were prepared by digesting PCR products amplified with the primer sets EGFP-Xb-F/EGFP-Xh-R and ggs1-Xh-F/ggs1-No-R using pPN97 and wild-type cDNA as templates, respectively.

Plasmid pSS41 (*DsRed-SKL*) containing the standard PTS1 motif SKL was prepared for co-localization studies. This plasmid was prepared by cloning into pSS37 a 0.69-kb *Xba*I/*Not*I fragment containing the *DsRed* coding region with the added SKL tripeptide in frame at its C-terminus. The *Xba*I/*Not*I fragment was prepared by digesting a PCR product amplified with the primer set DsRed-XbaI-F and SKL-No-R using pPgpd-DsRed (Mikkelsen et al. 2003) as template. Plasmid pSS37 was prepared by cloning into pSF16.17 a 1.45-kb *Sal*I/*Bgl*II fragment containing the *TEF* promoter of *Aureobasidium pullulans* (Vanden Wymelenberg et al. 1997) and the *trpC* terminator of *Aspergillus nidulans* (Mullaney et al. 1985). The 1.45-kb fragment was prepared by digesting a PCR product amplified with the primer set PTEF-SalI-F and TtrpC-BglII-R using pPN94 as template. Plasmid pSF16.17 was prepared by cloning a 1.7-kb fragment containing *nptII* under the control of the *trpC* promoter and terminator into the *Hpa*I site of pSP72 (Promega). Plasmids pSS46 (*EGFP-GRV*) and pSS54 (*EGFP-N368PaxG*) were prepared to study the subcellular localization of truncated PaxG. Plasmid pSS46 was prepared by cloning into pPN94 a 0.73-kb *Xba*I/*Not*I fragment containing the *paxG* C-terminus tripeptide GRV in frame at the C-terminus of the *EGFP* coding region. The *Xba*I/*Not*I fragment was prepared by digesting a PCR product amplified with the primer set EGFP-Xb-F and GRV-No-R using pPN97 as template. Plasmid pSS54 was prepared by cloning into pPN94 a 1.84-kb *Bam*HI/*Not*I fragment containing the coding regions of *EGFP* and truncated *paxG* cDNA, deleted for the last 9 bases coding the C-terminus tripeptide GRV. The *Bam*HI/*Not*I fragment was prepared by digesting a PCR product amplified with the primer set EGFP-Xb-F/CpaxG-dGRV-No-R using pSS28 as template.

paxG 'knockout' plasmid pSS52 was prepared by sequentially cloning into pSF15.15 a 1.04-kb *Sal*I/*Hin*dIII fragment 5′ of *paxG* and a 1.0-kb *Eco*RV/*Sac*I fragment 3′ of *paxG* from pSS16 (Saikia et al. 2006). The *Sal*I/*Hin*dIII fragment was prepared by digesting a PCR product amplified with the primer set paxGKO-Sal and paxGKO-Hin using wild-type genomic DNA as template. Plasmid pSF15.15 was prepared by cloning a 1.4-kb *Hin*dIII fragment containing *hph* under the control of the *trpC* promoter from pCB1004 (Carroll et al. 1994) into the *Sma*I site of pSP72. Δ*paxG* complementation plasmid pSS75 was prepared by cloning into pII99 (Namiki et al. 2001) a 1.93-kb *Hin*dIII/*Xho*I fragment containing the full-length *paxG*, together with 0.55-kb 5′ and 0.09-kb 3′ of *paxG*. The 1.93-kb fragment was prepared by digesting a PCR product amplified with the primer set paxG-HiC and paxG-XhC using pSS8 (Saikia et al. 2006) as template.

Plasmids pSS64 (*PaxG*), pSS65 (*GgsA*), and pSS66, pSS68 and pSS89 (truncated derivatives of *GgsA*) were prepared for GGPP synthase assay in *E. coli*. Plasmid pSS64 was prepared by cloning a 1.13-kb *Bam*HI/*Xho*I fragment containing *paxG* cDNA into pGEX-6P-3 (Amersham

Table 2 List of primers cited in this study

Primer name	Sequence (5′-3′)
paxG-Sp-F	GCACTAGTATGTCCTACATCCTTGC
paxG-Xh-R	ACTCGAGAACTCTTCCTTTCTC
EGFP-Xh-F	ATCTCGAGGTGAGCAAGG
EGFP-No-R	AGCGGCCGCTTACTTGTAC
EGFP-Xb-F	GTCTAGAATGGTGAGCAAGGG
EGFP-Xh-R	TCTCGAGCTTGTACAGCTCGTC
paxG-Xh-F2	GCTCGAGTCCTACATCCTTGCAGA
paxG-No-R2	GCGGCCGCTTAAACTCTTCCTTTCTC
ggs1-Xb-F	CCTCTAGAATGAGTTCTTCCTTTC
ggs1-Xh-R	ACTCGAGTTGGGCACCTTCATC
ggs1-Xh-F	CCTCGAGAGTTCTTCCTTTCAACC
ggs1-No-R	TGCGGCCGCCTATTGGGCAC
DsRed-Xbal-F	TCTAGAATGGCCTCCTCCGAGGAC
SKL-No-R	GCGGCCGCTTACAGCTTGCTCAGGAAC
PTEF-Sall-F	GTCGACGGTAGCAAACGGTGGTC
TtrpC-Bglll-R	CCGGCAGATCTATTGTATACCC
GRV-No-R	GCGGCCGCTTAAACTCTTCCCTTGTACAG
CpaxG-dGRV-No-R	GCGGCCGCTTATTTCTCATTAGTAGGG
paxGKO-Sal	CATCGTCGACTTCTAGCACCTGCAC
paxGKO-Hin	GAAAAGCTTCGAACCTCCATTGGC
paxG-HiC	TAAGCTTGGGTTGAAAAACGCCTGG
paxG-XhC	TCTCGAGATTCACGACCTGTGACTAGTC
PaxG-Ba–F	TGGATCCATGTCCTACATCCTTGC
PaxG-Xh-R2	TCTCGAGCTAAACTCTTCCTTTCTC
Ggs1-Ba–F	TGGATCCATGAGTTCTTCCTTTCAACCACC
Ggs1-Xh-R2	TCTCGAGCTATTGGGCACCTTCATC
d34Ggs1-Ba–F	TGGATCCATGTCCGTTACCGATGAACC
d71Ggs1-Ba–F	GCGGATCCATGAATGAGAAAATCCTGATGG
d79Ggs1-Ba–F	GCGGATCCATGTATGACTATATGCACCAGC
paxGNcF	CGCCATGGCTACATCCTTGCAGAAGC
paxGKpR	GCGGGTACCTTAAACTCTTCCTTTCTC
N368paxGKpR	GCGGGTACCTTATTTCTCATTAGTAGGG
ggs1NcF	CCACCATGGGTTCTTCCTTTCAAC
ggs1SKLKpR	CCGGTACCCTACAGCTTGCTTTGGGCACCTTCATC
C304ggs1NcF	GCCATGGATGAGAAAATCCTGATGGGC

Biosciences). The 1.13-kb fragment was prepared by digesting a PCR product amplified with the primer set PaxG-Ba–F and PaxG-Xh-R2 using pSS28 as template. Plasmid pSS65 was prepared by cloning a 1.14-kb *Bam*HI/*Xho*I fragment containing *ggsA* cDNA into pGEX-6P-3. The 1.14-kb fragment was prepared by digesting a PCR product amplified with the primer set Ggs1-Ba–F and Ggs1-Xh-R2 using pSS29 as template. Plasmid pSS66 was prepared by cloning into pGEX-6P-3 a 1.04-kb *Bam*HI/*Xho*I fragment containing truncated *ggsA* cDNA deleted for the first 102 bases. The 1.04-kb fragment was prepared by digesting a PCR product amplified with the primer set d34Ggs1-Ba–F and Ggs1-Xh-R2 using pSS29 as template. Plasmid pSS68 was prepared by cloning into pGEX-6P-3 a 0.93-kb *Bam*HI/*Xho*I fragment containing truncated *ggsA* cDNA deleted for the first 213 bases. The 0.93-kb fragment was prepared by digesting a PCR product amplified with the primer set d71Ggs1-Ba–F and Ggs1-Xh-R2 using pSS29 as template. Plasmid pSS89 was prepared by cloning into pGEX-6P-3 a 0.91-kb *Bam*HI/*Xho*I fragment containing truncated *ggsA* cDNA deleted for the first 237 bases. The 0.91-kb fragment was prepared by digesting a PCR product amplified with the primer set d79Ggs1-Ba–F and Ggs1-Xh-R2 using pSS30 as template.

Plasmids pSS110 (*PaxG*) and pSS111 (*N368PaxG*) were prepared to study the importance of the PaxG C-terminus

tripeptide in localization and in paxilline biosynthesis. Plasmid pSS110 was prepared by cloning a 1.30-kb *Nco*I/*Kpn*I fragment containing the full-length *paxG* into pPN1851 that contains the *paxM* promoter (Young et al. 2006). The *Nco*I/*Kpn*I fragment was prepared by digesting a PCR product amplified with the primer set paxGNcF and paxGKpR using wild-type genomic DNA as template. Plasmid pSS111 was prepared by cloning into pPN1851 a 1.29-kb *Nco*I/*Kpn*I fragment containing truncated *paxG* deleted for the last 9 bases encoding the GRV tripeptide. The *Nco*I/*Kpn*I fragment was prepared by digesting a PCR product amplified with the primer set paxGNcF and N368paxGKpR using wild-type genomic DNA as template. Plasmids pSS112 (*GgsA-SKL*) and pSS113 (*C304GgsA-SKL*) were prepared to examine if *ggsA*, targeted to peroxisome, could complement a Δ*paxG* strain for paxilline biosynthesis. Plasmid pSS112 was prepared by cloning into pPN1851 a 1.23-kb *Nco*I/*Kpn*I fragment containing the full-length *ggsA* with 9 additional bases, encoding the SKL tripeptide, in frame at its C-terminus. The *Nco*I/*Kpn*I fragment was prepared by digesting a PCR product amplified with the primer set ggs1NcF and ggs1SKLKpR using wild-type genomic DNA as template. Plasmid pSS113 was prepared by cloning into pPN1851 a 1.01-kb *Nco*I/*Kpn*I fragment containing truncated *ggsA* deleted for the first 213 bases but with 9 additional bases, encoding the SKL tripeptide, in frame at its C-terminus. The *Nco*I/*Kpn*I fragment was prepared by digesting a PCR product amplified with the primer set C304ggs1NcF and ggs1SKLKpR using wild-type genomic DNA as template.

Carotenoid biosynthesis assay

For in vivo GGPP synthase assay, *E. coli* BL21 (DE3) (Studier and Moffatt 1986) cells harboring the plasmid pACCAR25ΔcrtE (Sandmann et al. 1993), which contains all the carotenoid biosynthesis genes except for *crtE* encoding GGPP synthase, were transformed with each chimeric pGEX-6P-3 plasmid and plated on LB agar plates containing ampicillin (100 μg/ml) and chloramphenicol (20 μg/ml). Resistant colonies were re plated on LB agar plates containing the same antibiotics and incubated at 37°C for 16 h in dark. The change in the color of the colonies due to the accumulation of carotenoids was examined.

P. paxilli transformation

Protoplasts of *P. paxilli* and its derivatives were prepared as described previously (Saikia et al. 2006). Transformants were selected on regeneration medium supplemented with either hygromycin (100 μg/ml) or geneticin (150 μg/ml) (Roche Applied Science).

Indole-diterpene analysis

Fungal mycelium was analyzed for indole-diterpenes by reverse-phase HPLC as described previously (Saikia et al. 2006). In reverse-phase HPLC analysis, the characteristic feature of an indole moiety showing an absorption maximum at 230 nm and an absorption minimum at 280 nm was employed to confirm the presence of an indole-diterpene in a sample. However, all reverse-phase HPLC traces reported in this study are shown for 230 nm wavelength.

DNA sequencing and bioinformatics

DNA fragments were sequenced by the dideoxynucleotide chain-termination method (Sanger et al. 1977) using BigDye (Version 3) chemistry (PerkinElmer Life Sciences) with oligonucleotide primers (Sigma Genosys). Products were separated on an ABI Prism 377 sequencer (PerkinElmer Life Sciences). DNA sequences were assembled into contigs using Sequencher™ 4.2.2 (Gene Codes Corporation) and annotated and diagrammatically represented using either MacVector™ 7.2.3 (Accelrys) or Discovery Studio Gene version 1.5 (Accelrys).

Microscopy

Samples were prepared by inoculating 1 μl of 10^6 conidia on PD agar or PD agar supplemented with oleic acid mounted on a sterile microscopic slide and incubating at 22°C for approximately 2 days. After incubation, 10% glycerol was added to the sample before microscopy.

For staining with MitoTracker® Red CMXRos (Molecular Probes) and FM 4-64 (Molecular Probes), mycelia suspension was prepared by inoculating 10^6 conidia in 1 ml of PD broth and incubating at 22°C with shaking at 150 rpm for approximately 2 days. Mycelia were stained with 0.1 mM MitoTracker and 10 mM FM 4-64 by incubating for 30 min at 22°C with shaking at 150 rpm in dark. After incubation, mycelia were pelleted by centrifugation at 13,000 rpm for 1 min and washed twice in PD broth at 13,000 rpm for 1 min. The pellet was re suspended in 50 μl of 10% glycerol and a 10 μl aliquot was transferred to a microscopic slide for microscopy. For staining with Hoechst (Invitrogen), 10 μl of 1 M Hoechst was applied directly on the fungal colony and incubated for 2 min in the dark before microscopy.

Fungal mycelia were observed with an Olympus BX51 fluorescence microscope using a FITC filter for EGFP fluorescence, a CY3 filter for MitoTracker and FM 4-64 fluorescence and a DAPI filter for Hoechst fluorescence. All images were captured at 100× magnification with a MagnaFire™ digital camera and software (Optronics). The

images were stored as TIF files and processed with Canvas 10 software (ACD Systems International).

Results

GGPP synthases in filamentous fungi

Previous studies have shown that the filamentous fungus *P. paxilli* contains two proteins GgsA and GgsB (PaxG) that have significant amino acid sequence similarity to *Neurospora crassa* Al-3, a GGPP synthase in the carotenoid biosynthesis pathway (Young et al. 2001). A BLASTP analysis using PaxG sequence as a query identified homologous sequences in other filamentous fungi including *A. flavus*, *A. fumigatus*, *A. nidulans*, *A. niger*, *A. oryzae*, *F. fujikuroi*, *F. graminearum*, *Magnaporthe grisea*, *N. lolii* and *N. crassa*. These proteins all contain five conserved regions, including the two aspartate-rich domains DDXX(XX)D and DDXXD, found in all *trans*-prenyltransferases that catalyze the sequential addition of IPP to allylic prenyl diphosphates, forming precursors for both primary and secondary metabolites. *paxG* was found to be associated with a gene cluster for the biosynthesis of the secondary metabolite paxilline (Young et al. 2001). Like *paxG*, *atmG* in *A. flavus*, *ltmG* in *N. lolii* and *ggs2* in *F. fujikuroi* are associated with secondary metabolite gene clusters for aflatrem, lolitrem and gibberellin biosynthesis, respectively (Tudzynski and Holter 1998; Young et al. 2005; Zhang et al. 2004). Phylogenetic analyses of all these sequences revealed two distinct groups (Fig. 1). One group contained PaxG-related sequences and the other GgsA-related sequences. The sequences within the PaxG group were more divergent than those within the GgsA group. Aligned GGPP synthase sequences from all these filamentous fungi show greatest variation among the sequences at their N-terminal region (Supplementary Figure 1). This variability suggests that the N-terminal region could harbor specific signals including those for protein targeting. Analysis of these sequences using PSORT II (Nakai and Horton 1999) identified peroxisomal targeting signals in PaxG and its homologues in *A. flavus*, *A. nidulans*, *A. niger*, *A. oryzae* and *F. graminearum* (Fig. 1 and Supplementary Figure 1; labeled red). The PaxG C-terminus tripeptide Gly–Arg–Val (GRV) appears to be a variation of the PTS1 motif SKL (Aitchison et al. 1991; Gould et al. 1989). This same analysis predicted GgsA and its homologue in *M. grisea* (Fig. 1; labeled green) as mitochondrial proteins. The N-terminal sequence of GgsA is represented mostly by the amino acids Ser, Ala and Arg and lacks the negatively charged amino acids Asp and Glu, features characteristic of mitochondrial targeting peptides (Emanuelsson et al. 2000).

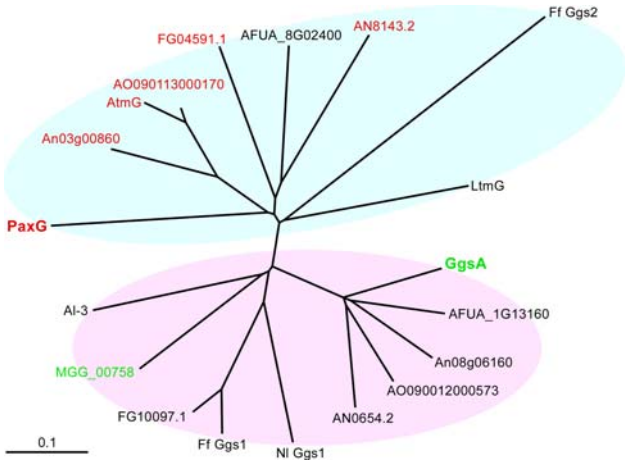

Fig. 1 An unrooted phylogenetic tree of GGPP synthases from filamentous fungi calculated by the neighbor joining method. Proteins predicted to be peroxisomal or mitochondrial are labeled *red* or *green*, respectively. *P. paxilli* PaxG and GgsA are in *bold*. The accession numbers of the corresponding sequences are as follows: *P. paxilli* PaxG, AAK11531, GgsA, AAK11525; *A. flavus* AtmG, AAT65717; *A. fumigatus* AFUA_8G02400, EAL84928, AFUA_1G13160, EAL90648; *A. nidulans* AN8143.2, EAA59165, AN0654.2, EAA65430; *A. niger* An03g00860, CAK38059, An08g06160, CAK45586; *A. oryzae* AO090113000170, BAE63215, AO090012000573, BAE60729; *F. fujikuroi* Ff Ggs2, CAA75568, Ff Ggs1, CAA65644; *F. graminearum* FG04591.1, EAA72205, FG10097.1, EAA68323; *M. grisea* MGG_00758, EDK02589; *N. crassa* Al-3, P24322; *N. lolii* LtmG, AAW88510, Nl Ggs1, AAW88513

P. paxilli paxG and *ggsA* encode GGPP synthases

Previously, PaxG and GgsA were assigned the GGPP synthase function based on *in silico* analysis (Young et al. 2001). In this study, we tested if PaxG and GgsA have GGPP synthase activity by using a carotenoid biosynthesis assay. This assay was done by co transforming *E. coli* BL21 (DE3) cells that do not possess GGPP synthase with plasmid pACCAR25Δ*crtE* (Sandmann et al. 1993) harboring all the carotenoid biosynthesis genes except for *crtE* (GGPP synthase) and plasmid pSS64 (*paxG*) or pSS65 (*ggsA*). The transformants were then screened for the formation of yellow colored colonies/cultures characteristic of carotenoid production. Both gave transformants that produced the expected yellow pigment (Fig. 2) confirming that *paxG* and *ggsA* encode functional GGPP synthases.

P. paxilli paxG is involved in secondary metabolism

Since the Δ*paxG* mutant strain reported earlier (Young et al. 2001) was subsequently found to also contain a deletion in the adjacent *paxA* gene (B. Monahan, S. Saikia and B. Scott, unpublished results) associated with the paxilline biosynthesis gene cluster, a *paxG* 'knockout' construct, pSS52, was made (Fig. 3a). *P. paxilli* wild-type strain

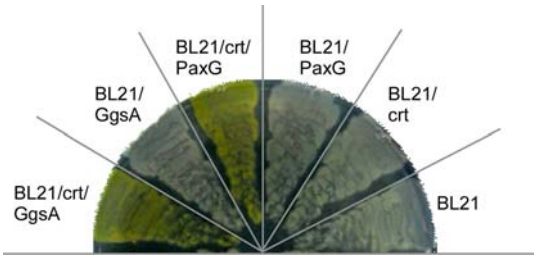

Fig. 2 *P. paxilli* PaxG and GgsA are GGPP synthases. *E. coli* BL21 (DE3) carrying pACCAR25ΔcrtE (crt) was transformed with pSS64 (*paxG*) or pSS65 (*ggsA*); plated on LB medium supplemented with ampicillin and chloramphenicol; and incubated at 37°C for 16 h. Both *paxG* and *ggsA* are under the control of the *E. coli tac* promoter

PN2013 was transformed with a PCR-generated linear fragment of pSS52 that resulted in about 100 hygromycin-resistant transformants. PCR screening of 42 arbitrarily selected spore-purified transformants identified 12 transformants that had patterns characteristic of targeted replacement events (data not shown). Southern analysis of *Pvu*II-digested genomic DNA of these 12 transformants and the wild-type, probed with the linear *paxG* 'knockout' fragment, confirmed that 6 transformants had a single copy integration of the construct at the *paxG* locus (Fig. 3b; shown for the Δ*paxG* mutant strain SSG2). The Δ*paxG* mutant strains had the same vegetative and conidiation phenotype as the wild-type.

We next examined if the deletion of *paxG* has any effect on paxilline biosynthesis. Extracts of SSG2 mycelia grown under paxilline producing conditions were analyzed by reverse-phase HPLC. No paxilline or any indole-diterpene intermediates were found in the extracts (Fig. 3c). Further, to confirm the function of *paxG*, a complementation construct, pSS75, containing the wild-type *paxG* under the control of the native promoter was prepared and transformed into the Δ*paxG* mutant strain SSG2. Consequently, production of paxilline and some intermediates were restored (Fig. 3c), confirming that *paxG* is required for paxilline biosynthesis. The presence of *ggsA* in this mutant background failed to restore paxilline biosynthesis suggesting subcellular compartmentalization of the two GGPP synthases.

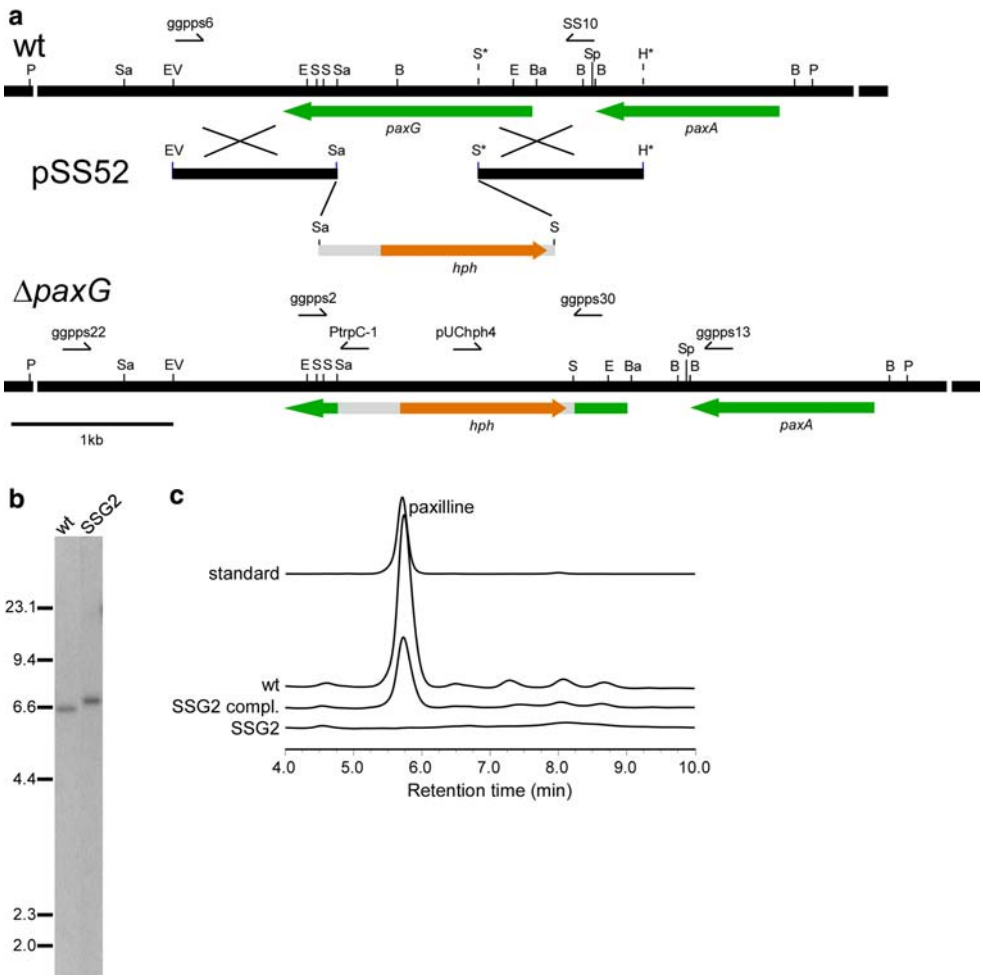

Fig. 3 Deletion analysis of *P. paxilli paxG*. **a** Physical map of the *P. paxilli paxG* wild-type (wt) genomic region, linear insert of *paxG*-replacement construct pSS52 and *P. paxilli paxG*-deletion mutant (Δ*paxG*) genomic region, showing the primers used for amplifying the linear replacement construct (primers ggpps6 & SS10) and screening gene integrations (primers ggpps2 & ggpps30, ggpps22 & PtrpC-1 and ggpps13 & pUChph4), and the restriction enzyme sites for *Bam*HI (Ba), *Bgl*II (B), *Eco*RI (E), *Eco*RV (EV), *Hin*dIII (H), *Pvu*II (P), *Sac*I (Sa), *Sal*I (S), and *Spe*I (Sp). The restriction sites marked by an *asterisk* are introduced by PCR for cloning. **b** Autoradiograph of a DNA gel blot of *Pvu*II genomic digests (1 μg) of *P. paxilli* wild-type (wt) and Δ*paxG* mutant strain SSG2 (PN2662) probed with [^{32}P]-labeled *paxG*-replacement construct, amplified from pSS52 with primers ggpps6 and SS10. **c** Reverse-phase HPLC analysis of mycelia extracts of *P. paxilli* Δ*paxG* mutant strain SSG2 (PN2662), SSG2 derivative strain (PN2663) (SSG2 compl.) and wild-type (wt)

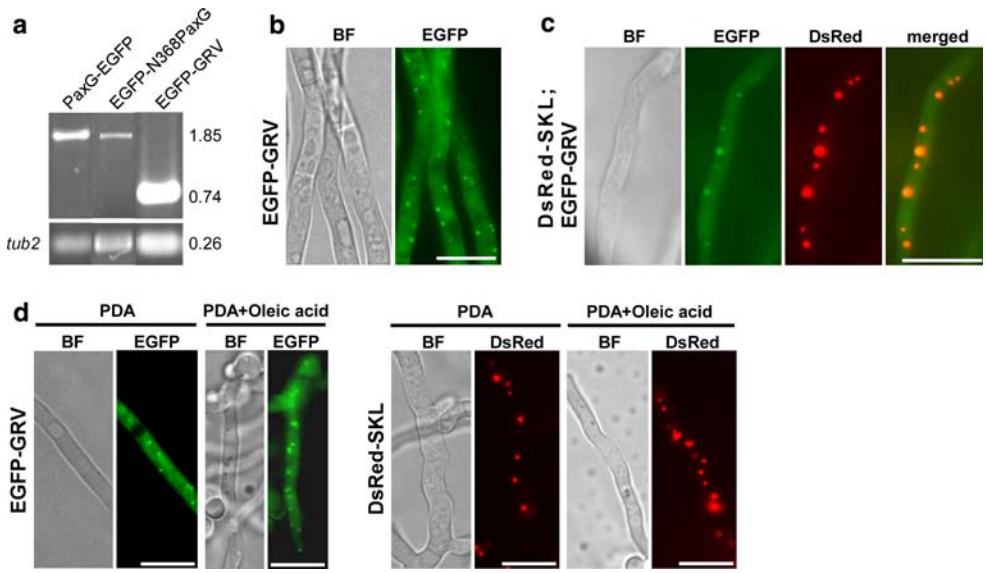

Fig. 4 The PaxG C-terminus tripeptide GRV is a peroxisomal targeting sequence. **a** Expression analysis of *PaxG-EGFP*, *EGFP-N368PaxG* and *EGFP-GRV* strains. RT-PCR analysis of total RNA isolated from 6 day old mycelia of *P. paxilli* wild-type derivative strains PN2559, PN2731 and PN2564 containing the fusion constructs pSS27 (*PaxG-EGFP*), pSS54 (*EGFP-N368PaxG*) and pSS46 (*EGFP-GRV*), respectively. These strains were confirmed by Southern to contain the respective chimeric genes. *Numbers* on the *right* correspond to the fragment sizes indicated in kb. **b** EGFP-GRV fusion protein is localized to punctuate organelles. *P. paxilli* wild-type derivative strain PN2564 containing the fusion construct pSS46 (*EGFP-GRV*) was grown on PD agar at 22°C for 2 days. Bright Field (BF) and EGFP fluorescence images of the mycelium are shown. **c** EGFP-GRV fusion co-localizes with DsRed-SKL fusion in punctuate organelles (peroxisomes). *P. paxilli* wild-type derivative strain PN2570 containing both the fusion constructs pSS41 (*DsRed-SKL*) and pSS46 (*EGFP-GRV*) was grown on PD agar at 22°C for 2 days. Bright Field (BF), EGFP and DsRed fluorescence images, and merged images of EGFP and DsRed images of the mycelium are shown. **d** Oleic acid induces proliferation of the punctuate organelles (peroxisomes) containing the EGFP-GRV or DsRed-SKL fusions. *P. paxilli* wild-type derivative strains PN2564 and PN2566 containing the fusion constructs pSS46 (*EGFP-GRV*) and pSS41 (*DsRed-SKL*), respectively, were grown on PD agar or PD agar + 5 mM oleic acid at 22°C for 2 days. Bright Field (BF), EGFP and DsRed fluorescence images of mycelia are shown. All the reporter gene constructs are under the control of the *A. pullulans TEF* promoter and *A. nidulans trpC* terminator. *Bars* = 10 μM

PaxG C-terminus tripeptide GRV a peroxisomal targeting signal

PaxG has the tripeptide GRV at its C-terminus that is predicted to be a variant of the PTS1 motif SKL (Gould et al. 1989; Nakai and Horton 1999). To examine where PaxG is localized in the fungal cell, both N- and C-terminal EGFP fusions of PaxG cDNA were expressed under the control of the constitutively expressing *A. pullulans TEF* promoter (Vanden Wymelenberg et al. 1997). No stable transformants were obtained when *EGFP-PaxG* fusion construct (pSS28) was introduced into the wild-type protoplasts. While stable transformants expressing *PaxG-EGFP* fusion construct (pSS27) were obtained (Fig. 4a), no EGFP fluorescence was observed (data not shown). Southern blot analysis of these strains confirmed that the plasmid integrated ectopically with variable copy numbers (data not shown). We therefore transformed the wild-type protoplasts with *EGFP-GRV* fusion construct (pSS46), containing the PaxG C-terminus PTS1-like motif GRV, and also with *EGFP-N368PaxG* fusion construct (pSS54), containing the truncated PaxG deleted for its C-terminus tripeptide GRV. Similar to *PaxG-EGFP* expressing transformants, transformants expressing *EGFP-N368PaxG* fusion construct (Fig. 4a) did not exhibit EGFP fluorescence (data not shown). However, transformants containing *EGFP-GRV* fusion were stable and expressed the fusion protein in punctuate organelles (Fig. 4a, b). To test if the punctuate organelles expressing the *EGFP-GRV* fusion are peroxisomes, an *EGFP-GRV* strain was transformed with a *DsRed-SKL* fusion construct (pSS41) containing the standard PTS1 motif SKL and examined by microscopy. Co-localization of DsRed-SKL and EGFP-GRV fusion proteins to the same organelles was observed (Fig. 4c). This result provides strong evidence that the EGFP-GRV-located organelles are peroxisomes.

Since oleic acid is known to induce peroxisome proliferation (Maggio-Hall et al. 2005; Valenciano et al. 1996; Veenhuis et al. 1987; Yan et al. 2005), both *EGFP-GRV* and *DsRed-SKL* strains, when grown on PD medium supplemented with oleic acid, showed a marked increase in the number of organelles containing the fusion proteins, as a result of oleic acid treatment (Fig. 4d). This result further supports the hypothesis that the punctuate organelles

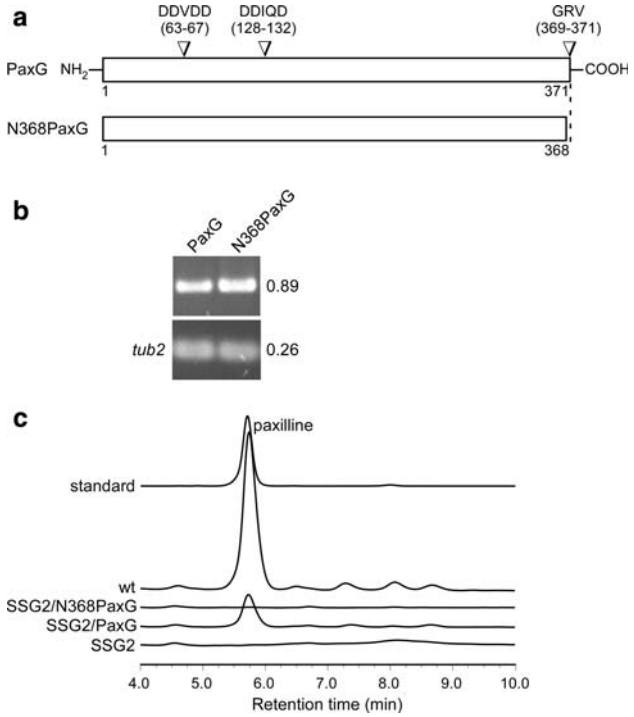

Fig. 5 Truncated PaxG, without the C-terminus tripeptide, does not complement the Δ*paxG* mutant strain SSG2 for paxilline biosynthesis. **a** C-terminal truncated version of the *paxG* ORF. *Numbers* indicate amino acid residues. **b** Expression analysis of SSG2 derivative strains containing PaxG or N368PaxG under the control of the *P. paxilli paxM* promoter. RT-PCR analysis of total RNA isolated from 6 day old mycelia of *P. paxilli* SSG2 derivative strains PN2664 and PN2665 containing the constructs pSS110 (PaxG) and pSS111 (N368PaxG), respectively. These strains were confirmed by PCR to contain the respective genes. *Numbers* on the *right* correspond to the fragment sizes indicated in kb. **c** Reverse-phase HPLC analysis of mycelia extracts of *P. paxilli* Δ*paxG* mutant strain SSG2 (PN2662), SSG2 derivative strains PN2664 (SSG2/PaxG) and PN2665 (SSG2/N368PaxG), and wild-type (wt)

containing the EGFP-GRV and DsRed-SKL fusions are peroxisomes. Together, these data suggest that PaxG is localized to the peroxisomes.

We next examined whether proper localization of the PaxG protein by its C-terminus tripeptide is important for paxilline biosynthesis. To test this hypothesis, complementation constructs encoding full-length PaxG (pSS110) and a C-terminal deletion derivative N368PaxG (pSS111; Fig. 5a), were each introduced into the Δ*paxG* mutant strain SSG2. Reverse-phase HPLC analysis of the extracts of the strains expressing the respective genes (Fig. 5b) showed that while the full-length PaxG was able to complement for paxilline biosynthesis the C-terminal deletion derivative N368PaxG could not (Fig. 5c). This result indicates that the PaxG C-terminus tripeptide GRV is functionally important for paxilline biosynthesis presumably due to correct organelle localization.

Subcellular localization of *P. paxilli* GgsA

PSORT II analysis predicts that GgsA is a mitochondrial protein. To test the localization of GgsA protein, constitutively expressing N- and C-terminal EGFP fusions of GgsA cDNA, *EGFP-GgsA* (pSS30) and *GgsA-EGFP* (pSS29), were each introduced into the wild-type protoplasts. While the *EGFP-GgsA* expressing strain (Fig. 6a) showed predominant cytoplasmic localization of the fusion protein (data not shown), the *GgsA-EGFP* expressing strain (Fig. 6a) showed localization of the fusion protein in punctuate organelles (Fig. 6b). Southern analysis of these strains confirmed the presence of at least one copy of the respective integrating constructs (data not shown). Microscopy analysis of a *GgsA-EGFP* strain transformed with the *DsRed-SKL* fusion construct showed discrete localization of the two fusion proteins to different organelles (Fig. 6c) suggesting that the GgsA-EGFP-located organelles are not peroxisomes. In addition, the mitochondrial specific dye MitoTracker® Red CMXRos stained organelles (mitochondria) other than the GgsA-EGFP-located punctuate organelles (Fig. 6d) confirming that these organelles are not mitochondria. Furthermore, the nuclei specific dye Hoechst, stained organelles (nuclei) other than those that fluoresced with the GgsA-EGFP construct (Fig. 6e), confirming that the latter are not nuclei. The membrane-selective fluorescent dye FM 4-64 also stained organelles (vacuoles) that were not GgsA-EGFP-located organelles (Fig. 6f).

Identification of truncated GgsA with GGPP synthase activity

Given, GgsA is unable to complement the PaxG function for paxilline biosynthesis in the Δ*paxG* mutant background, we tested if GgsA targeted to peroxisomes, by addition of the standard PTS1 motif SKL at its C-terminus, would complement the PaxG function. Given, the putative N-terminal signal peptide might override the effect of the PTS1 motif introduced at the C-terminus of GgsA, N-terminal truncated GgsA mutants C341GgsA (pSS66), C304GgsA (pSS68) and C296GgsA (pSS89; Fig. 7a) were first tested for GGPP synthase activity by the carotenoid biosynthesis assay. Based on this assay, C341GgsA and C304GgsA exhibited GGPP synthase activity similar to full-length GgsA; C296GgsA did not exhibit GGPP synthase activity (Fig. 7b). Since the C304GgsA exhibited GGPP synthase activity, it was selected for introducing the PTS1 motif SKL at its C-terminus. Although, subsequent introduction of C304GgsA-SKL (pSS113) and GgsA-SKL (pSS112) fusion constructs into the Δ*paxG* mutant strain SSG2 gave transgenic strains expressing the respective transcripts (Fig. 8a), both constructs failed to complement for paxilline biosynthesis (Fig. 8b).

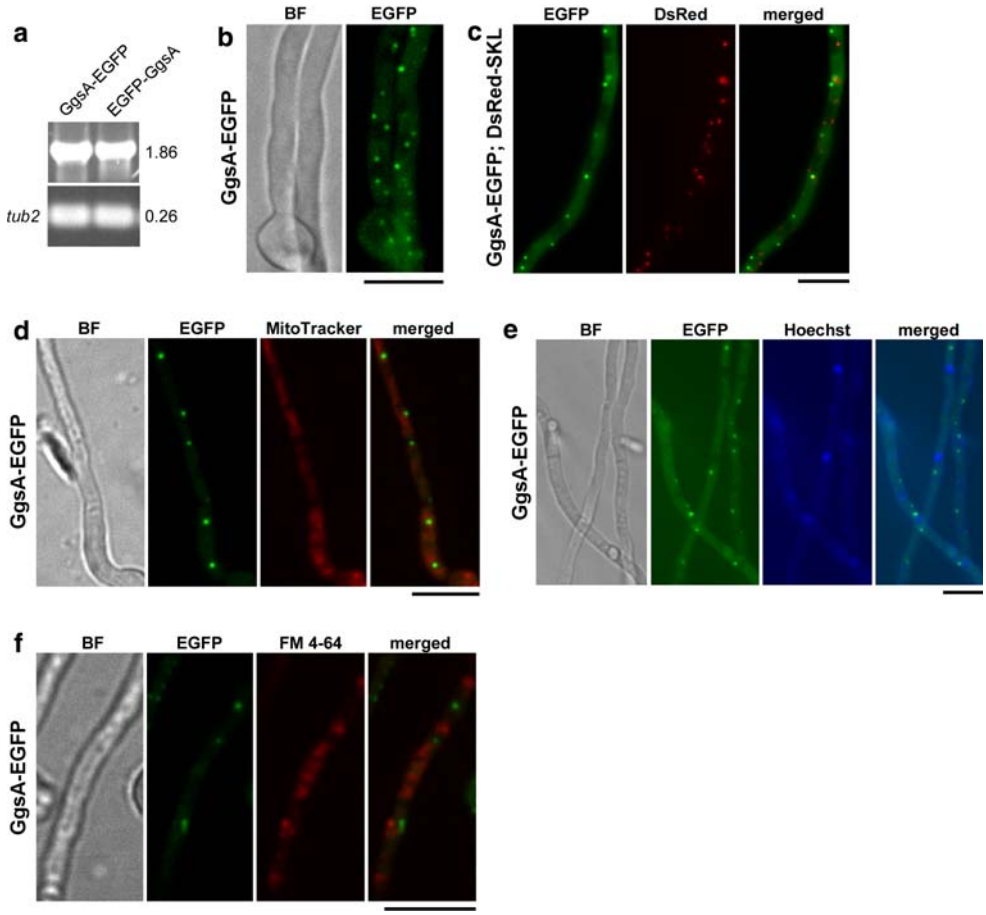

Fig. 6 GgsA is localized to punctuate organelles. **a** Expression analysis of *GgsA-EGFP* and *EGFP-GgsA* strains. RT-PCR analysis of total RNA isolated from 6 day old mycelia of *P. paxilli* wild-type derivative strains PN2555 and PN2549 containing the fusion constructs pSS29 (*GgsA-EGFP*) and pSS30 (*EGFP-GgsA*), respectively. These strains were confirmed by Southern to contain the respective fused genes. *Numbers* on the *right* correspond to the fragment sizes indicated in kb. **b** GgsA-EGFP fusion protein localizes to punctuate organelles. *P. paxilli* wild-type derivative strain PN2555 containing the fusion construct pSS29 (*GgsA-EGFP*) was grown on PD agar at 22°C for 2 days. Bright Field (BF) and EGFP fluorescence images of the mycelium are shown. **c** GgsA-EGFP fusion protein does not co-localize with DsRed-SKL fusion. *P. paxilli* wild-type derivative strain PN2575 containing both the fusion constructs pSS29 (*GgsA-EGFP*) and pSS41 (*DsRed-SKL*) was grown on PD agar at 22°C for 2 days. EGFP and DsRed fluorescence images, and merged images of EGFP and DsRed images of the mycelium are shown. Organelles containing the GgsA-EGFP fusion protein are not stained with MitoTracker (**d**), Hoechst (**e**) and FM 4-64 (**f**). *P. paxilli* wild-type derivative strain PN2555 containing the fusion construct pSS29 (*GgsA-EGFP*) was grown in PD broth at 22°C with shaking at 150 rpm for 2 days. Mycelia were than stained with 0.1 mM MitoTracker® Red CMXRos or 10 mM FM 4-64 for 30 min in the same growth medium. Bright Field (BF), EGFP fluorescence, MitoTracker and FM 4-64 staining images, and merged images of EGFP and MitoTracker staining images and EGFP and FM 4-64 staining images of the mycelium are shown. All the reporter gene constructs are under the control of the *A. pullulans TEF* promoter and *A. nidulans trpC* terminator. *Bars* = 10 μM

Discussion

In this study, we investigated the subcellular localization of the two *P. paxilli* GGPP synthases, GgsA and PaxG and also the role of PaxG in secondary metabolism. Based on a carotenoid biosynthesis assay, we found that *paxG* and *ggsA* encode proteins that have GGPP synthase activities. Deletion and complementation analyses confirmed that *paxG* is essential for paxilline biosynthesis in *P. paxilli*. Our reporter fusion studies demonstrated that the EGFP-GRV fusion protein, containing the PaxG C-terminus tripeptide GRV, was targeted to peroxisomes and that the GgsA-EGFP fusion protein was targeted to punctuate organelles of unknown identity. Further, the functional analysis of truncated PaxG mutants confirmed that the PaxG C-terminus tripeptide GRV is indispensable for paxilline biosynthesis.

The primary structures of GGPP synthases from different filamentous fungi vary at their N-terminal region suggesting that this region could harbor specific signals for protein targeting. Although detailed information on localization of fungal GGPP synthases is not available, GGPP synthases

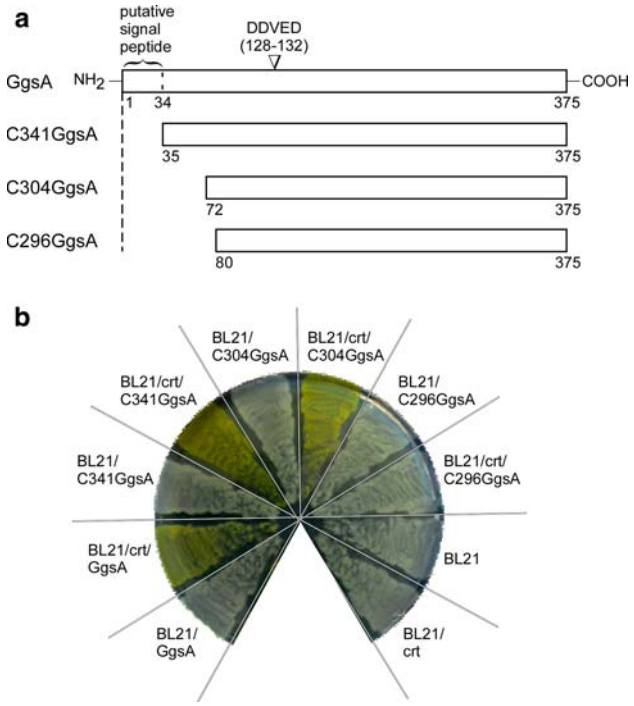

Fig. 7 Truncated versions of the *ggsA* ORF retain GGPP synthase activity. **a** N-terminal truncated versions of the *ggsA* ORF. *Numbers* indicate amino acid residues. **b** Putative N-terminal signal sequence of the *ggsA* ORF is dispensable for GGPP synthase activity. *E. coli* BL21 (DE3) carrying pACCAR25ΔcrtE (crt) was transformed with pSS66 (C341GgsA), pSS68 (C304GgsA) or pSS89 (C296GgsA); plated on LB medium supplemented with ampicillin and chloramphenicol; and incubated at 37°C for 16 h. All truncated versions of the *ggsA* ORF are under the control of the *E. coli tac* promoter

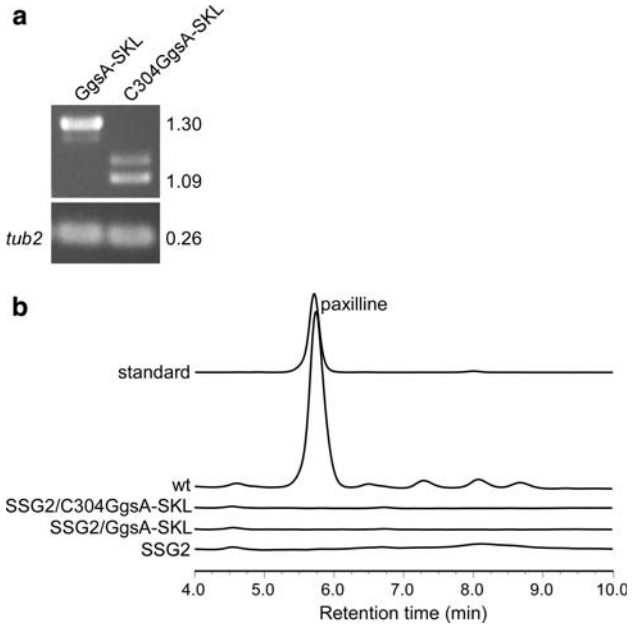

Fig. 8 Full-length and truncated versions of *ggsA* ORF with the added PTS1 motif SKL do not provide the *paxG* function for paxilline biosynthesis. **a** Expression analysis of SSG2 derivative strains containing *GgsA-SKL* and *C304GgsA-SKL* under the control of the *P. paxilli paxM* promoter. RT-PCR analysis of total RNA isolated from 6 day old mycelia of *P. paxilli* SSG2 derivative strains PN2666 and PN2667 containing the constructs pSS112 (*GgsA-SKL*) and pSS113 (*C304GgsA-SKL*), respectively. These strains were confirmed by PCR to contain the respective genes. *Numbers* on the *right* correspond to the fragment sizes indicated in kb. **b** Reverse-phase HPLC analysis of mycelia extracts of *P. paxilli* Δ*paxG* mutant strain SSG2 (PN2662), SSG2 derivative strains PN2666 (SSG2/GgsA-SKL) and PN2667 (SSG2/C304GgsA-SKL), and wild-type (wt)

with putative localization signals at their N-terminal regions have been reported in plants (Okada et al. 2000; Sitthithaworn et al. 2001; Zhu et al. 1997). GgsA is predicted to contain a mitochondrial targeting peptide at its N-terminus. Our analysis of GgsA, with both N- and C-terminal EGFP fusions, showed that a free GgsA N-terminus is not absolutely necessary but is required for efficient targeting of the GgsA protein to punctuate organelles. These punctuate organelles, to which the GgsA-EGFP fusion protein was targeted, were not mitochondria, peroxisomes, nuclei or vacuoles, as shown by our dual labeling and cellular staining studies. Unlike the punctuate shape of these organelles, mitochondria usually appear as tubular structures within hyphae, along the longitudinal axis of the cell (Inoue et al. 2002; Koch et al. 2003; Maggio-Hall and Keller 2004; Suelmann and Fischer 2000).

Deletion analysis, in conjunction with a carotenoid biosynthesis assay, showed that truncated GgsA still functions as a GGPP synthase. However, both full-length and truncated GgsA with the added PTS1 SKL motif at their C-terminus did not complement a Δ*paxG* mutant strain for paxilline biosynthesis. Possible explanations for this result could be that GgsA has a different allylic substrate to PaxG, synthesis of paxilline may require metabolic channeling facilitated by PaxG protein-protein interactions, or PaxG may have an additional role in paxilline biosynthesis besides synthesis of GGPP. Furthermore, to provide the function of PaxG, GgsA might require some motif that is only present in PaxG. One such candidate is a DDXDD motif present at the N-terminus of PaxG (Fig. 5a). Although this motif is not present in GgsA or in any other PaxG homologues reported in this study, a similar DXDD motif is a characteristic feature of type B diterpene cyclases that initiate cyclization of GGPP by protonation of the double bond (Kawaide et al. 2000).

PaxG contain the PTS1-like sequence (Aitchison et al. 1991; Gould et al. 1989)—and its homologues in *A. flavus*, *A. nidulans*, *A. niger*, *A. oryzae* and *F. graminearum* contain the peroxisomal targeting signal type 2 (PTS2)-like sequences (Petriv et al. 2004). The presence of either PTS1 or PTS2 suggests that these proteins may be localized to peroxisomes. In this study, we could not determine the precise subcellular localization of the full-length PaxG. This was because the EGFP-tagged full-length PaxG either

affected cell growth (EGFP-PaxG) or failed to fluoresce (PaxG-EGFP) suggesting that the constitutive expression of *EGFP-PaxG* was toxic to the cell, or the tertiary structure of the PaxG-EGFP fusion protein was affecting the fluorescence property of EGFP, respectively. However, three sets of evidence viz., co-localization, oleic acid induction and complementation studies confirmed that the PaxG C-terminus tripeptide GRV not only functions as a peroxisomal targeting signal but is also indispensable for paxilline biosynthesis.

It is interesting to note that some secondary metabolic pathway enzymes including that for AK-toxin in *A. alternata* (Tanaka et al. 1999; Tanaka and Tsuge 2000), penicillin in *P. chrysogenum* (Muller et al. 1991, 1992) and aflatoxin and sterigmatocystin in *Aspergillus* species (Maggio-Hall et al. 2005) are predicted/verified to be peroxisomal. These results establish a key role for this organelle in secondary metabolism. This could be either due to the ready availability of the substrate acetyl-CoA for diterpenes and polyketides or a mechanism to protect fungal cells from the potential deleterious effects of toxins like aflatoxins. Based on our data on apparent peroxisomal localization of PaxG, we propose that PaxG synthesizes GGPP from the precursors derived from acetyl-CoA in peroxisomes. However, subsequent paxilline biosynthesis steps could either occur in peroxisomes or in other organelles since subsequent indole-diterpene intermediates including paspaline, 13-desoxypaxilline and the α- and β-isomers of both PC-M6 and paxitriol, are readily transported across the membranes as demonstrated in our precursor-feeding studies (Saikia et al. 2007).

In conclusion, our studies on subcellular localization of *P. paxilli* GGPP synthases have given some insight into how the two proteins are compartmentalized. This initial study forms the basis for further work on localization of subsequent paxilline biosynthesis steps that could ultimately establish the importance of compartmentalization in diterpene secondary metabolism.

Acknowledgments We thank Aiko Tanaka (Nagoya University, Japan) for constructing pPN97, Simon Foster (The Sainsbury Laboratory, UK) for constructing pSF15.15 and pSF16.17, and Rohan Lowe (Rothamsted Research, UK) for constructing PN1775. We also thank Carolyn Young (The Samuel Roberts Noble Foundation, USA) for discussions on the phylogeny and alignment of GGPP synthases. This work was supported by a grant from the Royal Society of New Zealand (Marsden Grant MAU010). We thank Dmitry Sokolov from the Manawatu Microscopy and Imaging Centre for assistance with confocal microscopy.

References

Aitchison JD, Murray WW, Rachubinski RA (1991) The carboxyl-terminal tripeptide Ala–Lys–Ile is essential for targeting *Candida tropicalis* trifunctional enzyme to yeast peroxisomes. J Biol Chem 266:23197–23203

Carroll AM, Sweigard JA, Valent B (1994) Improved vectors for selecting resistance to hygromycin. Fungal Genet Newsl 41:22

Chen A, Kroon PA, Poulter CD (1994) Isoprenyl diphosphate synthases: protein sequence comparisons, a phylogenetic tree, and predictions of secondary structure. Protein Sci 3:600–607

Chiou CH, Lee LW, Owens SA, Whallon JH, Klomparens KL, Townsend CA, Linz JE (2004) Distribution and sub-cellular localization of the aflatoxin enzyme versicolorin B synthase in time-fractionated colonies of *Aspergillus parasiticus*. Arch Microbiol 182:67–79

Daum G, Lees ND, Bard M, Dickson R (1998) Biochemistry, cell biology and molecular biology of lipids of *Saccharomyces cerevisiae*. Yeast 14:1471–1510

Emanuelsson O, Nielsen H, Brunak S, von Heijne G (2000) Predicting subcellular localization of proteins based on their N-terminal amino acid sequence. J Mol Biol 300:1005–1016

Gould SJ, Keller GA, Hosken N, Wilkinson J, Subramani S (1989) A conserved tripeptide sorts proteins to peroxisomes. J Cell Biol 108:1657–1664

Inoue I, Namiki F, Tsuge T (2002) Plant colonization by the vascular wilt fungus *Fusarium oxysporum* requires *FOW1*, a gene encoding a mitochondrial protein. Plant Cell 14:1869–1883

Itoh Y, Johnson R, Scott B (1994) Integrative transformation of the mycotoxin-producing fungus, *Penicillium paxilli*. Curr Genet 25:508–513

Kawaide H, Sassa T, Kamiya Y (2000) Functional analysis of the two interacting cyclase domains in *ent*-kaurene synthase from the fungus *Phaeosphaeria* sp. L487 and a comparison with cyclases from higher plants. J Biol Chem 275:2276–2780

Koch KV, Suelmann R, Fischer R (2003) Deletion of *mdmB* impairs mitochondrial distribution and morphology in *Aspergillus nidulans*. Cell Motil Cytoskeleton 55:114–124

Kovacs WJ, Tape KN, Shackelford JE, Duan X, Kasumov T, Kelleher JK, Brunengraber H, Krisans SK (2007) Localization of the pre-squalene segment of the isoprenoid biosynthetic pathway in mammalian peroxisomes. Histochem Cell Biol 127:273–290

Lamas-Maceiras M, Vaca I, Rodriguez E, Casqueiro J, Martin JF (2006) Amplification and disruption of the phenylacetyl-CoA ligase gene of *Penicillium chrysogenum* encoding an aryl-capping enzyme that supplies phenylacetic acid to the isopenicillin N-acyltransferase. Biochem J 395:147–155

Lee LW, Chiou CH, Klomparens KL, Cary JW, Linz JE (2004) Subcellular localization of aflatoxin biosynthetic enzymes Nor-1, Ver-1, and OmtA in time-dependent fractionated colonies of *Aspergillus parasiticus*. Arch Microbiol 181:204–214

Lendenfeld T, Ghali D, Wolschek M, Kubicek-Pranz EM, Kubicek CP (1993) Subcellular compartmentation of penicillin biosynthesis in *Penicillium chrysogenum*. The amino acid precursors are derived from the vacuole. J Biol Chem 268:665–671

Maggio-Hall LA, Keller NP (2004) Mitochondrial β-oxidation in *Aspergillus nidulans*. Mol Microbiol 54:1173–1185

Maggio-Hall LA, Wilson RA, Keller NP (2005) Fundamental contribution of β-oxidation to polyketide mycotoxin production in planta. Mol Plant Microbe Interact 18:783–793

Mikkelsen L, Sarrocco S, Lubeck M, Jensen DF (2003) Expression of the red fluorescent protein DsRed-express in filamentous ascomycete fungi. FEMS Microbiol Lett 223:135–139

Mullaney EJ, Hamer JE, Roberti KA, Yelton MM, Timberlake WE (1985) Primary structure of the *trpC* gene from *Aspergillus nidulans*. Mol Gen Genet 199:37–45

Muller WH, van der Krift TP, Krouwer AJ, Wosten HA, van der Voort LH, Smaal EB, Verkleij AJ (1991) Localization of the pathway of the penicillin biosynthesis in *Penicillium chrysogenum*. EMBO J 10:489–495

Muller WH, Bovenberg RA, Groothuis MH, Kattevilder F, Smaal EB, Van der Voort LH, Verkleij AJ (1992) Involvement of microbodies in penicillin biosynthesis. Biochim Biophys Acta 1116:210–213

Nakai K, Horton P (1999) PSORT: a program for detecting sorting signals in proteins and predicting their subcellular localization. Trends Biochem Sci 24:34–35

Namiki F, Matsunaga M, Okuda M, Inoue I, Nishi K, Fujita Y, Tsuge T (2001) Mutation of an arginine biosynthesis gene causes reduced pathogenicity in *Fusarium oxysporum* f. sp. melonis. Mol Plant Microbe Interact 14:580–584

Okada K, Saito T, Nakagawa T, Kawamukai M, Kamiya Y (2000) Five geranylgeranyl diphosphate synthases expressed in different organs are localized into three subcellular compartments in *Arabidopsis*. Plant Physiol 122:1045–1056

Petriv OI, Tang L, Titorenko VI, Rachubinski RA (2004) A new definition for the consensus sequence of the peroxisome targeting signal type 2. J Mol Biol 341:119–134

Saikia S, Parker EJ, Koulman A, Scott B (2006) Four gene products are required for the fungal synthesis of the indole-diterpene, paspaline. FEBS Lett 580:1625–1630

Saikia S, Parker EJ, Koulman A, Scott B (2007) Defining paxilline biosynthesis in *Penicillium paxilli*: functional characterization of two cytochrome P450 monooxygenases. J Biol Chem 282:16829–16837

Sandmann G, Misawa N, Wiedemann M, Vittorioso P, Carattoli A, Morelli G, Macino G (1993) Functional identification of *al-3* from *Neurospora crassa* as the gene for geranylgeranyl pyrophosphate synthase by complementation with *crt* genes, in vitro characterization of the gene product and mutant analysis. J Photochem Photobiol B 18:245–251

Sanger F, Nicklen S, Coulson AR (1977) DNA sequencing with chain-terminating inhibitors. Proc Natl Acad Sci USA 74:5463–5467

Sitthithaworn W, Kojima N, Viroonchatapan E, Suh DY, Iwanami N, Hayashi T, Noji M, Saito K, Niwa Y, Sankawa U (2001) Geranylgeranyl diphosphate synthase from *Scoparia dulcis* and *Croton sublyratus.* Plastid localization and conversion to a farnesyl diphosphate synthase by mutagenesis. Chem Pharm Bull (Tokyo) 49:197–202

Southern EM (1975) Detection of specific sequences among DNA fragments separated by gel electrophoresis. J Mol Biol 98:503–517

Studier FW, Moffatt BA (1986) Use of bacteriophage T7 RNA polymerase to direct selective high-level expression of cloned genes. J Mol Biol 189:113–130

Suelmann R, Fischer R (2000) Mitochondrial movement and morphology depend on an intact actin cytoskeleton in *Aspergillus nidulans*. Cell Motil Cytoskeleton 45:42–50

Takemoto D, Tanaka A, Scott B (2006) A p67Phox-like regulator is recruited to control hyphal branching in a fungal-grass mutualistic symbiosis. Plant Cell 18:2807–2821

Tanaka A, Tsuge T (2000) Structural and functional complexity of the genomic region controlling AK-toxin biosynthesis and pathogenicity in the Japanese pear pathotype of *Alternaria alternata*. Mol Plant Microbe Interact 13:975–986

Tanaka A, Shiotani H, Yamamoto M, Tsuge T (1999) Insertional mutagenesis and cloning of the genes required for biosynthesis of the host-specific AK-toxin in the Japanese pear pathotype of *Alternaria alternata*. Mol Plant Microbe Interact 12:691–702

Tudzynski B, Holter K (1998) Gibberellin biosynthetic pathway in *Gibberella fujikuroi*: evidence for a gene cluster. Fungal Genet Biol 25:157–170

Valenciano S, Lucas JR, Pedregosa A, Monistrol IF, Laborda F (1996) Induction of β-oxidation enzymes and microbody proliferation in *Aspergillus nidulans*. Arch Microbiol 166:336–341

Vanden Wymelenberg AJ, Cullen D, Spear RN, Schoenike B, Andrews JH (1997) Expression of green fluorescent protein in *Aureobasidium pullulans* and quantification of the fungus on leaf surfaces. Biotechniques 23:686–690

Veenhuis M, Mateblowski M, Kunau WH, Harder W (1987) Proliferation of microbodies in *Saccharomyces cerevisiae*. Yeast 3:77–84

Verner K, Schatz G (1988) Protein translocation across membranes. Science 241:1307–1313

Yan M, Rayapuram N, Subramani S (2005) The control of peroxisome number and size during division and proliferation. Curr Opin Cell Biol 17:376–383

Yoder OC (1988) *Cochliobolus heterostrophus*, cause of southern corn leaf blight. Adv Plant Pathol 6:93–112

Young C, Itoh Y, Johnson R, Garthwaite I, Miles CO, Munday-Finch SC, Scott B (1998) Paxilline-negative mutants of *Penicillium paxilli* generated by heterologous and homologous plasmid integration. Curr Genet 33:368–377

Young C, McMillan L, Telfer E, Scott B (2001) Molecular cloning and genetic analysis of an indole-diterpene gene cluster from *Penicillium paxilli*. Mol Microbiol 39:754–764

Young CA, Bryant MK, Christensen MJ, Tapper BA, Bryan GT, Scott B (2005) Molecular cloning and genetic analysis of a symbiosis-expressed gene cluster for lolitrem biosynthesis from a mutualistic endophyte of perennial ryegrass. Mol Genet Genomics 274:13–29

Young CA, Felitti S, Shields K, Spangenberg G, Johnson RD, Bryan GT, Saikia S, Scott B (2006) A complex gene cluster for indole-diterpene biosynthesis in the grass endophyte *Neotyphodium lolii*. Fungal Genet Biol 43:679–693

Zhang S, Monahan BJ, Tkacz JS, Scott B (2004) Indole-diterpene gene cluster from *Aspergillus flavus*. Appl Environ Microbiol 70:6875–6883

Zhu XF, Suzuki K, Saito T, Okada K, Tanaka K, Nakagawa T, Matsuda H, Kawamukai M (1997) Geranylgeranyl pyrophosphate synthase encoded by the newly isolated gene *GGPS6* from *Arabidopsis thaliana* is localized in mitochondria. Plant Mol Biol 35:331–341